Preprints of the 21st IFAC World Congress (Virtual)
Berlin, Germany, July 12-17, 2020

Utilisation of the Controllable Inertial Morphing for Providing Spacecraft with Acrobatic Attitude Capabilities. ⋆

Pavel M.Trivailo * **Andreas Rittweger** ** **Stephan Theil** **

* *RMIT University, School of Engineering, GPO Box 2476V, Melbourne, VIC 3001 Australia (e-mail: pavel.trivailo@rmit.edu.au).*
** *German Aerospace Center (DLR), Institute of Space Systems, Robert-Hooke-Straße 7, 28359 Bremen, Germany (e-mail: andreas.rittweger@dlr.de)*

Abstract: The paper is exploring a new method of controlling of the attitude dynamics of the spacecraft with non-zero angular momentum, using deliberately applied changes to the spacecraft inertial properties, called inertial morphing (IM). This method does not employ classical gyroscopic devices, nevertheless it enables the spacecraft to perform various acrobatics manoeuvres, allowing interchanges between stable and unstable states. In one case scenario, it enables transformation of the stable spin into unstable flipping motion and establishment of the desired periods of the flips at various stages of the procedure. Special consideration is given to the selection of the controllable morphed parameters to impose the desired periods and patterns of the acrobatics. This paper exploits use of the unstable flipping motions of the systems and due to established mini-max relationships for the flipping periods, enables selection of the system parameters, maximizing or minimizing the values of the periods for faster (more agile) maneuvers. In the other scenario, IM is used to transfer the regular spin about one body axis into the regular spin about another nominated body axis. Numerous illustration cases are presented and application of the new enhanced capabilities are discussed in detail. For example, paper presents a scenario of the reconfiguration of the articulated spacecraft with its segments being inverted during the acrobatic procedure in the desired way, which may open new possibilities during the spacecraft operation, including re-boost and landing.

Keywords: Spacecraft, angular momentum, attitude dynamics, inertial morphing, regular spin, tumbling, flipping, period, control, acrobatics.

1. INTRODUCTION

A phenomenon of periodic flips of the rigid body, spun about its intermediate axis is attributed to the "Tennis Racquet Theorem" and is often called the "Dzhanibekov's Effect", named after V.A.Dzhanibekov, who discovered it in space in 1985 while observing flying spinning wing nuts. However, famous USA scientist-astronaut Owen Kay Garriott, even earlier, in 1973, has performed his experiments with boxed rigid objects and also observed the flipping patterns, associated with their spin, conceptually predicted by Beachley (1971). For more information, please, refer to Trivailo & Kojima (2019 RaES); Murakami (2016).

2. INTRODUCTION INTO INERTIAL MORPHING

It has been realised that if the spinning system is designed in a way, where the inertial properties could be changed in the desired way, using, for example, mechanical or electromagnetic means, than these controls could be used for manipulations with attitude dynamics of the system. For extensive discussions on the topic interested reader may refer to the following references: Trivailo & Kojima (2019 ISSFD); Trivailo & Kojima (2019 JSASS); Trivailo & Kojima (2018 IAC); Trivailo & Kojima (2017 IAC); Trivailo & Kojima (2017 ISSFD), Noack (2019).

These are some examples of the system, admitting IM: spacecraft, deploying solar arrays; system with linear motors to re-position concentrated masses; systems, releasing pre-constrained masses, etc. (Trivailo & Kojima (2019 ISSFD)).

One of the scenarios of application of the inertial morphing may involve stabilisation of the flipping motion: this task may have two conceptual solution, at the expense of gaining or loosing angular velocity of the predominant spin (see Trivailo & Kojima (2017 ISSFD)). In another case, IM can be used for initiation of the flipping motion on the system, being initially in the stable spin.

This paper presents two detailed cases on using controlled IM: (1) first example demonstrates controls, enabling spinning spacecraft to performing acrobatic 180° inversion and allowing to use the same thruster for boosting and braking stages; (2) second example shows 90° inversion, enabling transition of the spin about one body axis into the spin about another nominated orthogonal axis.

⋆ The authors acknowledge support of the RMIT University and DLR Institute of Space Systems.

3. ANALYSIS OF THE PERIODIC FLIPPING MOTIONS

3.1 General Equations for calculation of the period T

The period of the unstable flipping motion can be calculated, using Eq. (37.12) in page 154 from the reference by Landau (1988)):

$$T = 4K \sqrt{\frac{I_{xx}\, I_{yy}\, I_{zz}}{(I_{zz} - I_{yy})\,(H^2 - 2\,\mathcal{K}_0\, I_{xx})}} \tag{1}$$

where K is complete elliptic integral of the first kind

$$K = \int_0^1 \frac{ds}{\sqrt{(1-s^2)\,(1-k^2 s^2)}} = \int_0^{\pi/2} \frac{du}{\sqrt{1-k^2\,\sin^2 u}} \tag{2}$$

being a function of the parameter k^2

$$k^2 = \frac{(I_{yy} - I_{xx})(2\,\mathcal{K}_0\, I_{zz} - H^2)}{(I_{zz} - I_{yy})(H^2 - 2\,\mathcal{K}_0\, I_{xx})} \tag{3}$$

It should be noted that Eqs. (1)-(3) correspond to the case of $H^2 > 2\,\mathcal{K}_0\, I_{yy}$. If this condition is not observed, in Eqs. (1)-(3) subscripts "xx" and "zz" must be interchanged.

Eq.1 has been used (Trivailo & Kojima (2019 RaES)) to investigate selection of the value of the intermediate moment of inertia I_{yy} on the flipping period.

However, as the detailed analysis on the influence on the flipping period T of the angular velocity of the predominant spin ω_y (here we will assume, for the convenience in notations, that $I_{xx} < I_{yy} < I_{zz}$) and combinations of principal moments of inertia of the system, I_{xx}, I_{yy}, I_{zz} have not been performed yet, this aspect is explored in this paper.

3.2 Influence of the value of the angular velocity ω_y of the predominant spin on the period T

In this paper we consider systems with non-zero initial angular momentum H_0. In case of the system with predominant spin about its intermediate axis, the major contributors to H_0 are the ω_y and I_{yy}.

Using Eq. 1, we can represent T as a 3D surface plot, explaining influence on the $T(\omega_y, I_{yy})$ function of its two argument. The resultant plot is shown in Fig. 1. It clearly reveals the tendency of the periods to become very large, when I_{yy} is approaching to the I_{xx} or I_{zz}. However, the plot also reveals the ridge of high value of periods, being asymmetrically in between I_{xx} and I_{zz}. As surface gradient is very high in vicinity of the ridge, it should be avoided for practical implementations, because in this area T would be very sensitive to small changes in I_{yy}, which would make control of the system period impractical.

As an example, in Fig. 1 we also intersect the T surface with two illustrative level values of the period: T=30 s and T=50 s. The intersection lines show that for the desired value of the flipping period T, there are multiple matching combinations of ω_y and I_{yy}, however, if the goal of the selection is to minimise the spin rate, then, there may be two local minimum specific values of I_{yy}. Two contour lines

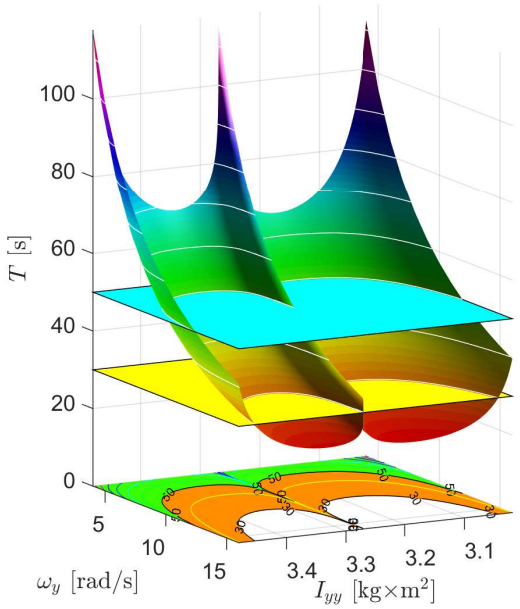

Fig. 1. Variation of the period $T(\omega_y, I_{yy})$ of the flipping motion with the changes in the predominant spinning angular velocity ω_y and value of the intermediate moment of inertia I_{yy} for the system with I_{xx}=3, I_{zz}=3.5 kg×m^2 (i.e. $\eta = 0.8571$).

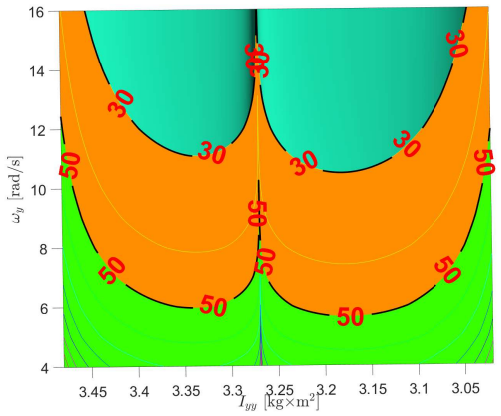

Fig. 2. Two labeled contour lines for the $T(\omega_y, I_{yy})$ surface in Fig. 1, corresponding to the values of the flipping periods equal to T=30 s and T=50 s.

for T=30 s and T=50 s are shown separately in Fig. 2. It shows, that, if, for example, the aim of the design process is to keep ω_y low, for the T=50, there are two solutions for I_{yy}, approximately equal to I_{yy}=3.335 and I_{yy}=3.18.

3.3 Influence of the value of the period T on the angular velocity ω_y of the predominant spin

Results in Fig. 1 are presented for the ω_y=$\omega_y(T, I_{yy})$, being a function of two arguments, T and I_{yy}. This function is shown Fig. 3 as a 3D surface plot. For the illustration purposes, we assume interest in two special values of angular velocity of the predominant rotation: ω_y=6 and ω_y=12 rad/s. The intersection lines of these level panes

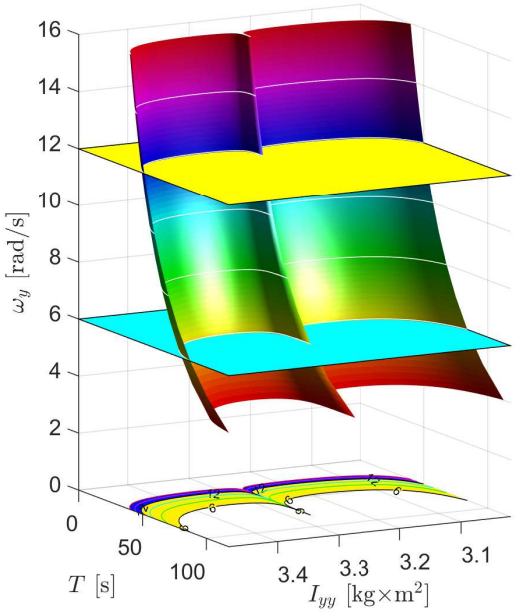

Fig. 3. Variation of the initial spin rate $\omega_y(T, I_{yy})$ with the changes in the period of the flipping motion T and value of the intermediate moment of inertia I_{yy} for the system with I_{xx}=3, I_{zz}=3.5 kg×m^2 (i.e. η=0.8571).

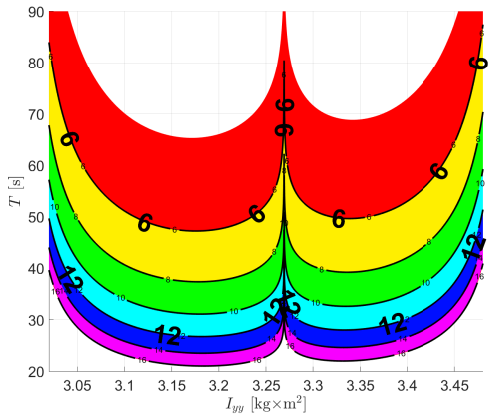

Fig. 4. Contour lines for the $T(\omega_y, I_{yy})$ surface in Fig. 3 with in-between bands individually colored. Red band corresponds to the ω_y=4–6 (rad/s) spin rate range; yellow band - to the ω_y=6–8 range; green band - to the ω_y=8–10, cyan band - to the ω_y=10–12 and blue band - to the ω_y=12–14 range and purple band - to the ω_y=14–16 range.

and the ω_y surface, together with other contour curves, are given in Fig. 4.

3.4 Numerical Simulation of the Systems with IM

In order to be able to simulate systems with IM, we need to extend Euler's equations, to allow variation in the moments of inertia of the system to be taken into consideration. These extended equations are:

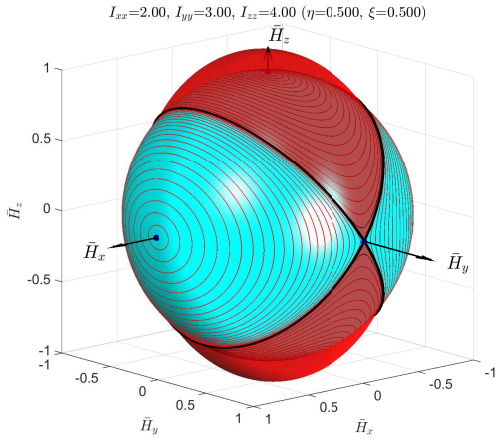

Fig. 5. Collocated Angular Momentum Sphere (light blue surface) and Kinetic Energy Ellipsoid (red surface), intersecting along the separatrices (shown with thick black lines).

$$\begin{bmatrix} \dot{I}_{xx} & 0 & 0 \\ 0 & \dot{I}_{yy} & 0 \\ 0 & 0 & \dot{I}_{zz} \end{bmatrix} \begin{Bmatrix} \omega_x \\ \omega_y \\ \omega_z \end{Bmatrix} + \begin{bmatrix} I_{xx} & 0 & 0 \\ 0 & I_{yy} & 0 \\ 0 & 0 & I_{zz} \end{bmatrix} \begin{Bmatrix} \dot{\omega}_x \\ \dot{\omega}_y \\ \dot{\omega}_z \end{Bmatrix} + + \begin{bmatrix} 0 & -\omega_z & \omega_y \\ \omega_z & 0 & -\omega_x \\ -\omega_y & \omega_x & 0 \end{bmatrix} \begin{bmatrix} I_{xx} & 0 & 0 \\ 0 & I_{yy} & 0 \\ 0 & 0 & I_{zz} \end{bmatrix} \begin{Bmatrix} \omega_x \\ \omega_y \\ \omega_z \end{Bmatrix} = \begin{Bmatrix} 0 \\ 0 \\ 0 \end{Bmatrix} \quad (4)$$

These equations can be solved numerically, using variety of methods. For details and examples of solutions, please, refer to Trivailo & Kojima (2017 ISSFD) and Trivailo & Kojima (2019 RaES).

3.5 Geometric Interpretation of Solutions

We employ graphical interpretation of the flipping motion, using angular momentum *unit sphere* (AMS) and kinetic energy ellipsoid (KEE), constructed in the non-dimensional coordinates of the normalised angular momentum H. The values of the semi-major axes of the ellipsoid are given with the following relationships:

$$a_x = q\sqrt{I_{xx}(t)}; \quad a_y = q\sqrt{I_{yy}(t)}; \quad a_z = q\sqrt{I_{zz}(t)}; \quad (5)$$
$$\text{where } q = \sqrt{K(t)}/H(0).$$

For the illustration system with $I_{xx} = 3$, $I_{xx} = 4$, and $I_{xx} = 5$, the AMS is shown with light blue color and KEE is shown with semi-transparent red ellipsoid. The line of intersection between both is known as polhoid and for the flipping case also corresponds to the separatrices, shown with thick black lines. Interestingly, that from Eq. 5 it follows that $a_z/a_x = \sqrt{I_{zz}/I_{xx}} = \sqrt{4/3} = 1.1547$, which explains the extend of the bulging of the part of the KEE over the AMS along the $\pm\bar{H}_z$ direction.

In our methodology, in order to perform fast and agile attitude transformations of the systems, we use IM to transfer the system into the state, when its angular momentum vector is sliding along the separatrix, therefore, we call this method "insertion into separatrix".

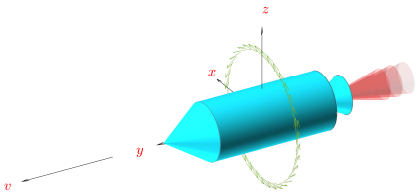

(a) Spacecraft is in stable y-axis spin: thruster is used for boost.

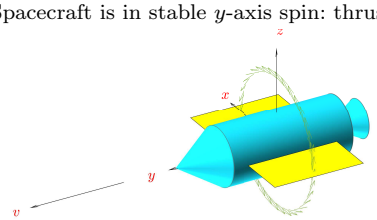

(b) Morphing-1 is activated to initiate y flips.

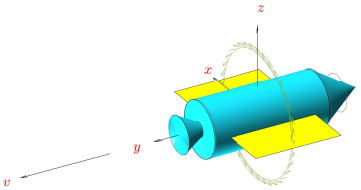

(c) 180 degrees y flip is completed.

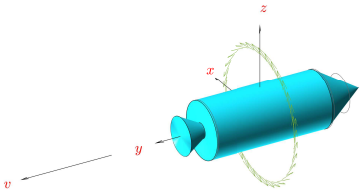

(d) Morphing-2 is activated to stop y flips.

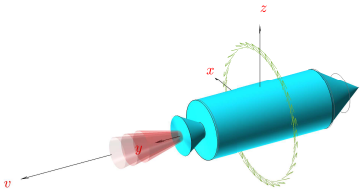

(e) Spacecraft is in stable y-axis spin: thruster is used for braking.

Fig. 6. Example of application of inertial morphing for inversion of the spacecraft, allowing to use the same thruster for the boosting and braking stages.

3.6 Application of Inertial Morphing: Detailed Example-1

Figure 6 is dedicated to one (out of many) possible applications of the IM. It illustrates inversion of the spacecraft, using two morphing procedures: the first is to activate unstable flipping motion and second is to stop flipping motion. This enables for a single thruster to be used for acceleration of the spacecraft (boosting stage, Fig. 6a) and also for its deceleration (braking stage, Fig. 6e).

To demonstrate the feasibility of the proposed application, let us consider six-masses model of the spacecraft with corresponding numerical parameters m_x=4 kg, m_y=5 kg; m_z=1 kg. The key requirement to this design would be ability of the system to re-position six paired masses (for example, via linear actuators), in accordance to the control considerations. Let us assume that the mission profile would enable installment of the spacecraft with initial predominant spin about y axis (with angular velocity ω_y = 8.57 and other components of ω being small: ω_x=ω_z=0.01,

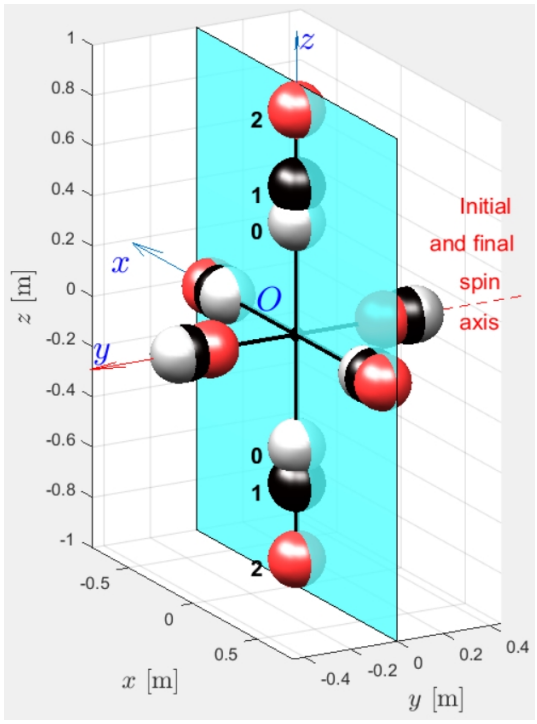

Fig. 7. Positions of the masses during spacecraft inversion via IM for acrobatic manoeuvre in Fig.6).

all in rad/s). If the masses are initially positioned at their locations, shown in Fig 7 with *white* spheres, with position radii equal to r_{x0}=548, r_{y0}= 510, and r_{z0}=447 mm correspondingly, then the inertial properties of the spacecraft would be $I_{xx,0}$=3; $I_{yy,0}$=2.8; $I_{zz,0}$=5 (all in kg×m^2). With these selected parameter, the y spin of the system would be stable, as axis of rotation coincides with the minimal inertia axis. Let assume that at the instant t=10 s we wish to initiate flipping motion of the system. This can be achieved by applying inertial "Morphing-1", during which moment of inertia I_{yy} should become an intermediate axis. Aiming for the new moments of inertia to be $I_{xx,1}$=3; $I_{yy,1}$=2.8; $I_{zz,1}$=5 (kg×m^2), we calculate new radii for the masses, using the following relationships:

$$\begin{aligned} I_{xx} &= 2\,(m_y\,r_y^2 + m_z\,r_z^2);\\ I_{yy} &= 2\,(m_z\,r_z^2 + m_x\,r_x^2);\\ I_{zz} &= 2\,(m_x\,r_x^2 + m_y\,r_y^2). \end{aligned} \tag{6}$$

Resultant values of the new position radii, ensuring transition of the system from stable regular spin to the flipping unstable motion are: r_{x1}=581, r_{y1}=480 and r_{z1}=592 mm. Therefore, to trigger the spinning motion, it is just necessary to move paired masses from initial positions (shown in Fig. 7 with white spheres) to their new positions, shown with *black* spheres. For better perception of the 3D design, an imagined semi-transparent xz plane is added to the figure. For the system, initially satisfying $I_{yy,0} < I_{xx,0} < I_{zz,0}$ condition, rapid assignment at t=10 s of the new moments of inertia, satisfying now $I_{xx,1} < I_{yy,1} < I_{zz,1}$ condition, transfers regular y spin motion into unstable spin. Its period can be calculated using Eq. 1 for the corresponding regular spin conditions at t=10 s: $I_{xx,1}$=3, $I_{yy,1}$=4.8, $I_{zz,1}$=5, ω_{x1}=-0.2917, ω_{y1}=5.0284, ω_{z1}=-0.6714. Calculations gives us T=17.784

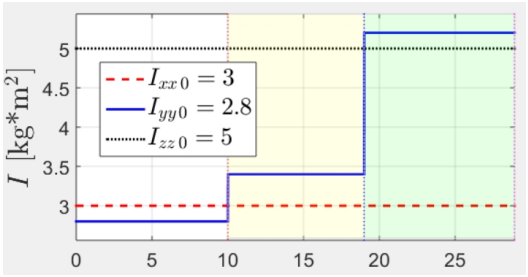

(a) time history of the spacecraft inertias I_{xx}, I_{yy}, I_{zz};

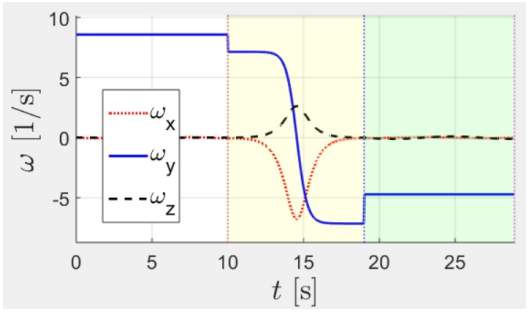

(b) time history of the angular velocities ω_x, ω_y, ω_z.

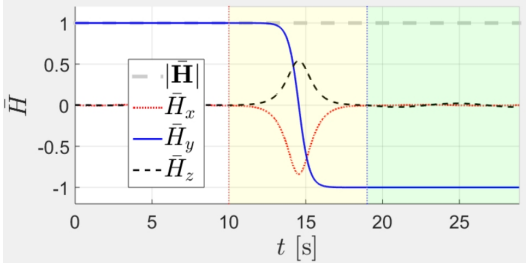

(c) time history of the angular momentum $\bar{\mathbf{H}}$ components.

Fig. 8. Realisation of the spacecraft "y"-axis inversion (shown in Fig.6) via two inertial morphings (as per Fig.7).

s, therefore, the time to 180° flip would be $T/2$=8.8920 s. At this very moment, rapid "Morphing-2" should be applied to stop flipping phase and stabilise the system. For this morphing, in accordance with Trivailo & Kojima (2017 ISSFD) any set of new moments of inertia can be selected, strictly satisfying any of the two conditions: $I_{yy,2} < I_{xx,2} < I_{zz,2}$ ("solution I_{yy} min" strategy) or $I_{xx,2} < I_{zz,2} < I_{yy,2}$ ("solution I_{yy} max" strategy). In one case scenario, return to the initial moments of inertia can be implemented. However, as an additional example, we illustrate implementation of the I_{xx}=3, I_{yy}=5.2, I_{zz}=5 ("solution-1" strategy) scenario. To achieve these new inertia characteristics, as per Eq. 6, spacecraft control masses should be rapidly moved to their final positions: r_{x2}=671, r_{y2}=374 and r_{z2}=894 mm. The the described morphings (achieved via controlled changes in $r_x(t)$, $r_y(t)$ and $r_z(t)$), time histories for the resulting moments of inertia, angular velocity and angular momentum components are presented in Fig. 8. Interestingly, that rapid changes in ω_y and I_{yy} do not lead to similar changes in $\bar{H}_y$. Also, as evidenced by Fig. 8c, the total angular momentum $|\bar{\mathbf{H}}|$ is conserved during the flipping acrobatics.

The same principle can be used for complete reconfiguration ("re-packaging") of the articulated compound spacecraft, consisting, for example, of three segments A_1-B_1, B_2-C_2, C_3-D_3. If all of these segments are un-docked, they can independently perform the same flipping maneuvre, as described above, then (after stabilisation) docked to a new configuration B_1-A_1, C_2-B_2, D_3-C_3. Note, that the re-configuration can be applied to the selected segments only and to the spacecraft with any number of segments. For example, if only central segment B_2-C_2 is inverted, the new configuration would be A_1-B_1, C_2-B_2, C_3-D_3.

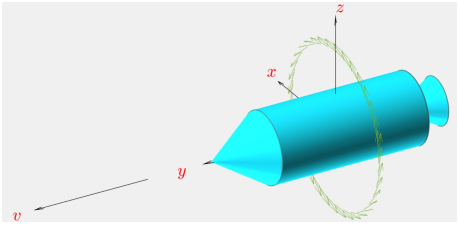

(a) Spacecraft is in stable spin about y body axis.

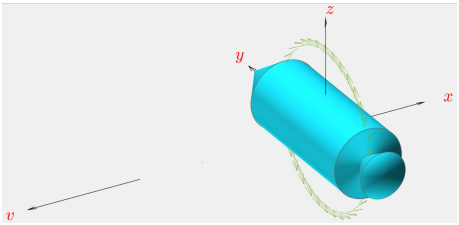

(b) Spacecraft is transferred to stable spin about x body axis.

Fig. 9. Example of application of inertial morphing for 90° change of the spin axis of the spacecraft.

3.7 Application of Inertial Morphing: Detailed Example-2

Figure 9 is dedicated to another possible applications of the IM. It illustrates 90° change of axis of spin of the spacecraft, using three morphing procedures: the first is to activate unstable flipping motion; second is to switch to x separatrix and the third is to stop tumbling motion with transfer of spacecraft spin from y to a new nominated *body* axis, being x in this illustration example. It should be noted, that in Fig. 10 initial and final spin axes are presented in *body* axis system. And in the global axis system, due to the law of conservation of angular momentum, both, initial and final spin orientations are aligned with the same direction of the angular momentum $|\bar{\mathbf{H}}|$ vector.

Spacecraft morphing parameters, corresponding to Fig.9-10, are shown in Table 1. Initially system is in stable spin (shown as IM0 in table). IM1 was designed to insert the system into "y" separatrix, similar to shown in Fig.5. This initiates a "y" flip, during which IM2 is applied, forcing the system to transfer to "x" separatrix. So, this acrobatics involves two "installments into separatrices". Important control consideration is: IM2 is applied at the instant when in body axes vector $|\bar{\mathbf{H}}|$ (to be displayed in boxy axes, as in Fig.5) passes *intersection* of "x" and "y" separatrices. IM3 is designed to stop "x" flips in the same way as shown in Fig.8.

4. CONCLUSION

This paper presents details of the new method of control of the attitude dynamics of the spacecraft, which does not require conventional gyroscopic devices, but instead

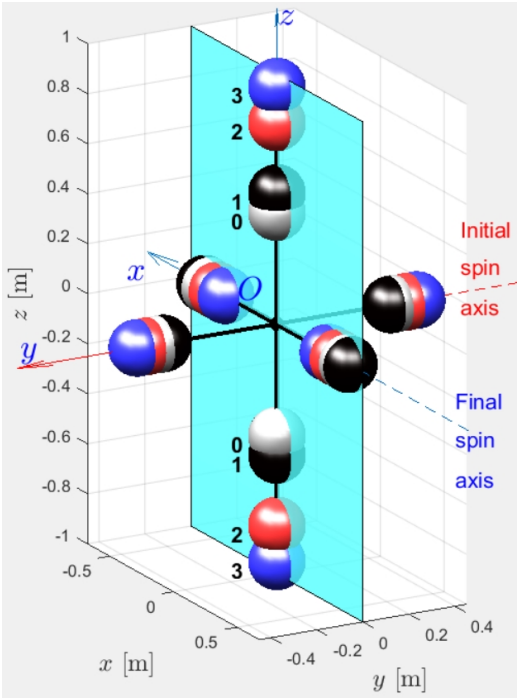

Fig. 10. Positions of the masses during spacecraft inversion via IM for acrobatic manoeuvre in Fig. 9.

is using inertial morphing. Resulting in a lighter and simple hardware implementation (with simple mechanical, electrical and/or magnetic devices, capable of changing the mass distribution of the system), it may be used on the smaller spacecraft. The key of the proposed efficient control method is in geometric interpretation of the changes of the kinetic energy ellipsoid of the system during applied inertial morphing. This interpretation enables determination of the controls for the desired transformation of the initial attitude motion into another type of motion with desired characteristics. This method exploits unstable flipping motion of the system, which occurs when the system is provided with the predominant spin about its intermediate axis of inertia. For the desired acrobatics, the system is deliberately transferred into the flipping mode with the pertinent separatrices, and then is switched to the new inertial properties at the instants, corresponding to the intersection with the separatrices, typically corresponding to different body axis, pertinent to the new desired flipping direction. After the transfer of one unstable flipping into another flipping is achieved, the motion can be further stabilised when the angular momentum vector reaches one of two pole positions. The paper also presents a method of selection of the morphing parameters to secure the flips with desired periods. To illustrate the application of the presented methodology, an articulated spinning spacecraft is considered. During the demonstration, its segments were disconnected, enabling some segments to perform inversions via flips with further inertial morphing stabilisation and finally consolidation of the spacecraft inverted components. This can be, for example, useful at the landing phase of the mission, when the instruments from the central part of the spacecraft are repositioned to the front.

Table 1. Spacecraft morphed parameters.

IM index	t s	r_1 mm	r_2 mm	r_3 mm	I_{xx} kg×m^2	I_{yy} kg×m^2	I_{zz} kg×m^2
0	0	548	510	447	3	2.8	5
1	10	565	495	524	3	3.1	5
2	18.25	474	566	806	4.5	3.1	5
3	25.15	403	608	949	5.5	3.1	5
f	35.14	403	608	949	5.5	3.1	5

REFERENCES

Trivailo, P.M. and Kojima, H. (2019). Enhancement of the Spinning Spacecraft Attitude Dynamics Capabilities using Inertial Morphing. *Royal Aeronautical Society The Aeronautical Journal*, 12:1–34.

Murakami, H., Rios, O. and Impelluso, T.J. (2016). A Theoretical and Numerical Study of the Dzhanibekov and Tennis Racket Phenomena. *Journal Applied Mechanics*, 83, (Sept. 08, 2016), No. 11, 111006 (10 pages). Paper No: JAM-16-1017, doi:10.1115/1.4034318.

Noack, D. (2019). In-Orbit Verification of a Fluid-Dynamic Attitude Control System. Paper 2019-d-041. *Proc. of the 32nd ISTS & 9th NSAT (The International Symposium on Space Technology and Science and Nano-Satellite Symposium)*, Fukui, Japan, 15-21 June 2019.

Trivailo, P.M., Kojima, H. (2019). Enhancement of the Spacecraft Attitude Dynamics Capabilities via Combination of the Inertial Morphing and Reaction Wheels (Keynote Paper and Presentation). [Peer Reviewed]. *Transactions of the 18th Australian International Aerospace Congress (AIAC2019), incorporating 27th International Symposium on Space Flight Dynamics (ISSFD)*. Engineers Australia, Royal Aeronautical Society. ISBN: 978-1-925627-21-3. Pp.1093-1122.

Trivailo, P.M., Kojima, H. (2019) Discovering Method of Control of the "Dzhanibekov's Effect" and Proposing its Applications for the Possible Future Space Missions. *Transaction of JSASS (The Japan Society for Aeronautical and Space Sciences), Aerospace Technology Japan*, 2019, Vol. 17, No. 1, pp. 72-81. DOI: 10.2322/tastj.17.72.

Trivailo, P.M. and Kojima, H. (2018) Augmented Control of Inversion of the Spinning Spacecraft, using Inertial Morphing, Paper IAC-18,C2,3,5,x45333, *Proc. of the 69th International Astronautical Congress (IAC)*, Bremen, Germany, 01-05 October 2018. 16 pp.

Trivailo, P.M. and Kojima, H. (2017). Re-Discovering "Dzhanibekov's Effect" Using Non-Linear Dynamics and Virtual Reality. Paper IAC-17,E1,7,10,x41083, *Proc. of the 68th International Astronautical Congress (IAC)*, Adelaide, Australia, 25-29 September 2017. IAC, Vol. 17, pp. 11394-11407, - 14 pp.

Trivailo, P.M. and Kojima, H. (2017). Utilisation of the "Dzhanibekov's Effect" for the Possible Future Space Missions. Paper ISTS-2017-d-047/ISSFD-2017-047, *Proc. of the Joint Conference: 31st ISTS, 26th ISSFD & 8th NSAT*, Matsuyama, Japan, 3-9 June 2017. - 10 pp.

Wie, B (2008). Space Vehicle Dynamics and Control. Second Edition, *AIAA Education Series*, 2008. 966 pp, doi:10.2514/4.860119.

Beachley, N. N. (1971). Inversion of Spin-Stabilized Spacecraft by Mass Translation - Some Practical Aspects. *Journal of Spacecraft*, 8, pp. 1078-1080.

Landau, L.D. and Lifshitz, E.M. (1988). *Mechanics*. Vol.1 (In Russian). - 4th ed. Moscow, "Nauka". - 216 pp.